Differential Space-Time Network Coding for Multi-Source Cooperative Communications

Zhenzhen Gao, *Student Member, IEEE*, Hung-Quoc Lai, *Member, IEEE*, and K. J. Ray Liu, *Fellow, IEEE*

Abstract—Due to the asynchronous nature of cooperative communications, simultaneous transmissions from two or more nodes are challenging in practice. The existing cooperative communications employing successive transmission from one user node to the other can avoid the synchronization problem but results in large transmission delay. In addition, channel estimation in multi-source cooperative communications is a challenging and costly task due to the amount of training, especially when the number of cooperative users is large. Considering these practical challenges in multi-source cooperative communications, this paper proposes a differential space-time network coding (DSTNC) scheme for narrowband multi-source cooperative communications to overcome the problems of imperfect synchronization and complex channel estimation without introducing large transmission delay. Each user in the network linearly combines the correctly decoded symbols via network coding and transmits its packet in time division multiple access (TDMA) mode. The pairwise error probability is analyzed and the design criteria of the DSTNC are derived to achieve full diversity. For broadband cooperative communications, distributed differential space-time-frequency network coding (DSTFNC), which is differentially encoded within each orthogonal frequency-division multiplexing (OFDM) block, is designed through mapping from the proposed DSTNC. When the statistical channel power-delay profile is known at the corresponding user node, each node can permutate its channel independently to improve the performance of the DSTFNC scheme. Simulation results are presented to verify the performance of the proposed schemes.

Index Terms—Multinode cooperative communications, synchronization, channel estimation, space-time network coding, space-time-frequency network coding.

I. INTRODUCTION

IT is well known that due to the fading effect, the transmission over wireless channels suffers from severe attenuation in signal strength. Spatial diversity is an attractive way to combat fading in wireless communications because it can be readily combined with other forms of diversity and still offer dramatic performance gains when other forms of diversity are unavailable [1]. Multiple-input multiple-output (MIMO) with space-time coding techniques exploit spatial diversity through multiple transmit and/or receive antennas [2]-[3]. However

Z. Gao and K. J. R. Liu are with the Department of Electrical and Computer Engineering, University of Maryland, College Park, MD 20742 USA (e-mail: {ygggzhen, kjrliu}@umd.edu). Z. Gao is also with the School of Electronic and Information Engineering, Xi'an Jiaotong University, Xi'an, China, 710049. This work was done during her visit to the University of Maryland.

H.-Q. Lai is with the US Army RDECOM CERDEC, RDER-STA-DS, Bldg. 242, Aberdeen Proving Ground, MD 21005 USA (e-mail: hungquoc.lai@us.army.mil).

with the required separation among antennas that is usually at least a half of wavelength, it is often impractical to equip multiple antennas for small size transceivers such as nodes in wireless sensor networks and mobile networks.

User cooperation is an effective scheme to introduce spatial diversity in wireless networks without the use of co-located multiple antennas. The distributed antennas from the relays form a virtual antenna array to provide spatial diversity. Most of the existing studies assume perfect synchronization and perfect channel state information (CSI) available at the destination [4], [5]. However, such an assumption is difficult to be met in practice. The cooperative diversity is provided by different antennas in separated terminals, where each terminal has its own local oscillator (LO). These LO's generate transmit frequencies with certain variations, and it is hard for the destination to estimate and compensate all the frequency offsets at once. The frequency synchronization issue becomes much worse when cooperative nodes are in mobile with different Doppler effects. It is also challenging for the destination to receive all relaying signals simultaneously due to different propagation time, processing time, and timing estimation errors. Besides, channel estimation is a challenging and costly task, especially in time-selective fading environments [6]. The amount of overhead becomes substantial in multi-source wireless systems because the amount of training or convergence time (incurred by blind techniques) grows with the number of links.

Recently, there have been studies on space-time coding for asynchronous cooperative systems to achieve full diversity. Coding methods that tolerate the timing synchronization errors are discussed in [7], and [8]. However, these schemes come with the additional overheads to accommodate the timing mismatches. In [9], intentional delays are introduced in different relay nodes, and minimum mean square error (MMSE) estimator is used at the destination to exploit the cooperative diversity. However, full diversity is not guaranteed. To achieve full diversity in frequency-selective channels without perfect synchronization, [10] proposed the randomized space-time codes, and [11] exploited the structure of time-reverse space-time block code (TR-STBC). Both of the transmissions are structured in blocks of appropriate length to eliminate inter-block interference. However, if space-time block codes are used in [10], the transmission rates of [10] and [11] decrease as the number of relays increases. Full-diversity multisource cooperation protocols have been proposed in [12] and [13] based on complex field coding to improve spectral efficiency. To reduce the transmission delay caused by traditional TDMA transmission, novel concepts of wireless network
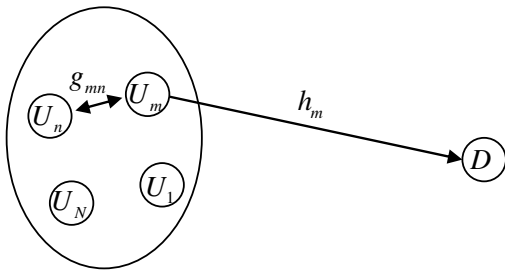
Fig. 1. Wireless multi-source cooperative communication network.

cocast (WNC) and space-time network coding (STNC) have been proposed by leveraging the idea of network coding in [14] and [15]. WNC in [14] can provide incremental diversity, while the STNC scheme in [15], which combines symbols in code division multiple access (CDMA) or frequency division multiple access (FDMA) mode at each relay, can solve the imperfect synchronization issue and achieve full diversity. $2N$ time slots are required by the STNC in [15] for a network of N nodes to transmit N packets. Compared to N^2 time slots for a traditional TDMA-based cooperative communication network of N nodes [5], this is a substantial reduction in transmission delay. However, in both [14] and [15], extra frequency resource is required.

All these asynchronous schemes have assumed CSI known at the receivers. However, as mentioned in previous part, channel estimation is challenging and often not possible in a fast-fading environment. To overcome the problem of channel estimation, differential encoding and modulation schemes for cooperative communications have been investigated, such as [16] and [17]. The differential scheme in [16] is based on space-time codes for MIMO systems, which would fail if the synchronization is imperfect. In [17], a single transmission with differential M-array phase shift keying (DMPSK) modulated symbols in TDMA manner can overcome the synchronization issue but causes large transmission delay. From the above discussion, there is a clear need of a cooperative communication scheme that can leverage the advantages of the discussed schemes while overcoming their shortages.

In this paper, we first propose a differential space-time network coding (DSTNC) scheme for narrowband cooperative communication systems to solve the issues of imperfect synchronization and channel estimation. By exploiting the idea of STNC in [15], TDMA is also used in this paper. The differential encoding is performed across the symbols within the same packet at each node. Different from the STNC in [15], a combining function, which is determined by a network coding vector, is designed in this paper for each node to reduce the transmission delay while achieving full diversity. Note that due to the adoption of FDMA or CDMA in [15], more bandwidth is needed by the STNC scheme to separate different users' signals. In our proposed DSTNC scheme, the same frequency band is used for the whole network and thus the proposed DSTNC scheme has higher spectral efficiency than the STNC in [15]. The network coding here, which

is a set of complex parameters optimized for conventional signal constellations, is different from the traditional network coding, which linearly combines Galois symbols with coding coefficients picked from a finite field of fixed size [18], [19]. We analyze the pairwise error probability (PEP) performance of the proposed DSTNC scheme and derive the diversity criterion and product criterion for the design of the DSTNC. It is verified by the simulations that full diversity can be achieved by the proposed DSTNC scheme.

For broadband cooperative communications, orthogonal frequency-division multiplexing (OFDM) is used at each user node. A distributed differential space-time-frequency network code (DSTFNC) is designed from the proposed DSTNC via mapping. The DSTFNC is differentially encoded over subcarriers within each OFDM block. Therefore, it can be decoded even the fading channels remain constant only within each OFDM block and may change independently from one OFDM block to another. When a statistical channel power-delay profile (PDP) is known at the corresponding user node, a smooth logical channel similar to [20] is created independently at each user node to improve the performance of the DSTFNC scheme. Simulation results show that the proposed DSTFNC scheme provides the expected full diversity even in some high mobility scenarios, where the channel may change within one OFDM block due to Doppler effects.

The rest of the paper is organized as follows. In Section II, system model and differential transmission for narrow-band cooperative communications are introduced. In Section III, the PEP performance is analyzed for frequency flat channels and the design of DSTNC is discussed. In Section IV, DSTFNC for broadband cooperative communications is generated from DSTNC and the permutation method for each node to create the smooth logical channel is illustrated when the corresponding PDP is known. In Section V, simulation results are shown to validate the proposed schemes. Finally, we draw our conclusions in Section VI.

Notations: Upper (lower) case boldface letters stand for matrices (vectors). $\otimes$ is the Kronecker product. T and H denote transposition and conjugate transposition of a matrix, respectively. E stands for expectation. $\|\mathbf{A}\|_F$ denotes the Frobenius norm of matrix $\mathbf{A}$. $\mathbf{I}_N$ is an $N \times N$ unit matrix. $\mathbf{0}_N$ and $\mathbf{1}_N$ are $N \times 1$ all-zero vector and all-one vector, respectively. $\text{diag}[d_1, \ldots, d_N]$ is the $N \times N$ diagonal matrix whose ith diagonal entry is d_i.

II. SYSTEM MODEL

Consider a wireless multi-source cooperative communication network depicted in Fig. 1, in which a set of N user nodes $U_i, 1 \leq i \leq N$, each equipped with a single antenna, cooperate to transmit their information to the destination node D. Without loss of generality, the transmitted information can be represented in terms of symbols. Nevertheless, the nodes will transmit packets that contains a large number of symbols. The destination will collect all the transmitted packets and then jointly detect the transmitted information as in the traditional network coding [18], [19]. Selective decode-and-forward protocol [1] is adopted in the cooperative communication network. For mathematical tractability, we
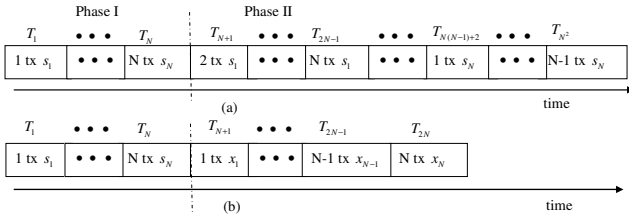
Fig. 2. Illustration of two-phase cooperative communications of repetition-based successive transmissions (a) and network coding transmissions (b).

Fig. 3. The construction of the DSTNC with the kth transmitted symbols of the N packets for narrowband cooperative communications.

assume that the relays can judge whether the received symbols are decoded correctly or not [5]. It is shown in [5] that this assumption is very close to the performance of practical scenario of comparing the received SNR to a threshold, especially when the nodes operate in high SNR, for example, when the nodes are close to each other. The channels between any two nodes in the network are modeled as narrow-band Rayleigh fading with additive white Gaussian noise (AWGN). Let g_{mn} and h_m denote the channel between U_m and U_n and the channel between U_m and D, $\forall m, n \in [1, N]$, respectively. Then g_{mn} and h_m are modeled as independent zero-mean, complex Gaussian random variables with variances $\mathrm{E}|g_{mn}|^2 = \sigma_{mn}^2$ and $\mathrm{E}|h_m|^2 = \sigma_m^2$, respectively. The channel variances are $\sigma_{mn}^2 = \kappa d_{mn}^{-\nu}$ and $\sigma_m^2 = \kappa d_m^{-\nu}$, where κ is a constant whose value depends on the propagation environment, d_{mn} and d_m is the distance between U_m and U_n and the distance between U_m and D, respectively, and ν is the path loss exponent, whose value is usually in the range between 2 and 4.

A. Transmission Model

Fig. 2 illustrates the transmission procedure for a two-phase cooperative communication. Each transmission period comprises two phases, the broadcasting phase (Phase I) and the encoding/relaying phase (Phase II). Assume that TDMA is used in each phase and frame synchronization has been established. In each phase, each node is assigned a time slot to transmit its packet, which contains a large number of symbols. The source nodes take turns to exchange their information in Phase I. In Phase II, unlike the traditional cooperative communication, where the nodes repeat the received packets, each node transmits a new packet, whose symbols are generated by combing the received symbols from different nodes with its network coding vector.

Fig. 3 illustrates the differential space-time network code with the kth symbols of the N packets in one transmission period. In Phase I, each user node $U_m, m \in [1, N]$, is assigned a time slot T_m to broadcast its packet to the rest of the user nodes with power P_I, where the kth transmitted symbol is v_m^k. In Phase II, each node transmits a new packet with power P_{II}, and the kth transmitted symbols of the packets are x_n^k, $n \in [1, N]$. Let $P_t = P_I + P_{II}$ be the total transmit power for a transmission. Assume that user nodes are far away from D, and the distance among the user nodes is small compared to the distance between the user nodes and D. A small P_I is enough for the transmission in Phase I. Thus there is no direct link between the use nodes and the destination node in Phase I.
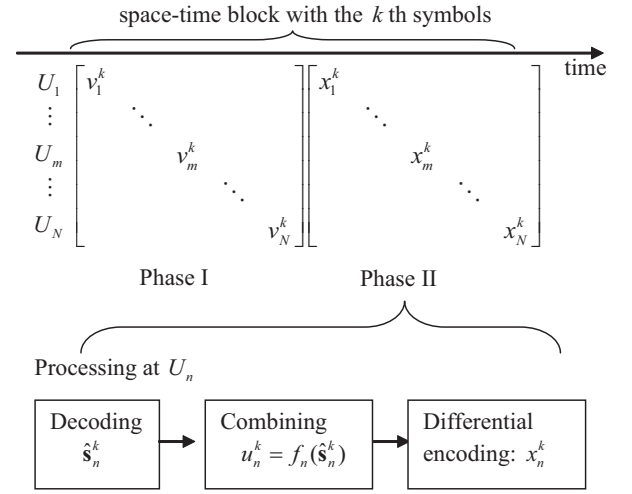
1) *Signal Transmission in Phase I:* Denote the kth information symbols of the N packets as a vector $\mathbf{s}^k = [s_1^k, s_2^k, ..., s_N^k]^{\mathrm{T}}$ with $k \in [0, N_s - 1]$, where N_s is the number of information symbols in a packet. The information symbol s_m^k of U_m, $m \in [1, N]$, is from an M-QAM constellation $\mathcal{A}$. Since no CSI is available at the user nodes, the transmitted symbol v_m^k in Phase I is differentially encoded as $v_m^k = s_m^k \frac{v_m^{k-1}}{|v_m^{k-1}|}$ with $k = 0$ denoting the initial reference symbol. The kth transmitted symbol of U_m received at U_n in Phase I can be written as

$$y_{mn}^k = \sqrt{P_I} g_{mn}^k v_m^k + w_{mn}^k, \qquad (1)$$

where w_{mn}^k is zero-mean and N_0-variance AWGN, g_{mn}^k is the channel between U_m and U_n during the transmission of v_m^k. After decoding, U_n obtains a set of estimated symbols $\hat{\mathbf{s}}_n^k = [\hat{s}_{1n}^k, ..., \hat{s}_{mn}^k, ..., \hat{s}_{Nn}^k]^{\mathrm{T}}$ from other nodes, where $\hat{s}_{mn}^k = \beta_{mn} s_m^k$ with β_{mn} indicating the detection state at U_n for s_m^k. β_{mn} for $m \neq n$ can be formulated as

$$\beta_{mn} = \begin{cases} 1, & \hat{s}_{mn}^k = s_m^k \\ 0, & \hat{s}_{mn}^k \neq s_m^k \end{cases}. \qquad (2)$$

It is obvious that $\beta_{nn} = 1$ due to the fact that U_n always has its own information. The detection states demonstrate that the user nodes just relay the symbols decoded correctly.

Then U_n combines the elements of the estimation $\hat{\mathbf{s}}_n^k$ using a linear function to form a unique symbol as follows

$$u_n^k = f_n(\hat{\mathbf{s}}_n^k) = \sum_{m=1}^{N} a_{mn} \hat{s}_{mn}^k = \mathbf{a}_n^{\mathrm{T}} \hat{\mathbf{s}}_n^k \qquad (3)$$

with $\mathbf{a}_n = [a_{1n}, ..., a_{nn}, ..., a_{Nn}]^{\mathrm{T}}$. Assume that $\mathbf{a}_n^{\mathrm{T}} \mathbf{a}_n = 1$. We call the combining factors $a_{mn}, m, n \in [1, N]$, as network coding coefficients and $\mathbf{a}_n$ as the network coding vector at U_n.

2) *Signal Transmission in Phase II:* Because the destination does not have CSI, each user node would transmit the combined symbol u_n^k differentially in Phase II, where $n \in [1, N], k \in [0, N_s - 1]$. The nodes transmit their packets in their assigned time slots, and the kth transmitted symbols

of the N packets can be written as a diagonal space-time matrix $\mathbf{D}_x^k = \mathrm{diag}[x_1^k, \ldots, x_n^k, \ldots, x_N^k]$, which is generated as follows

$$\mathbf{D}_x^k = \mathbf{D}_u^k \mathbf{D}_x^{k-1} \bar{\mathbf{D}}_x^{k-1}, \tag{4}$$

where $\mathbf{D}_x^{k-1} = \mathrm{diag}[x_1^{k-1}, \ldots, x_n^{k-1}, \ldots, x_N^{k-1}]$ represents the space-time block with the $(k-1)$th transmitted symbols of the N packets, $\mathbf{D}_u^k = \mathrm{diag}[u_1^k, \ldots, u_n^k, \ldots, u_N^k]$ is the information block with the kth combined symbols of the N users, and $\bar{\mathbf{D}}_x^{k-1} = \mathrm{diag}[\frac{1}{|x_1^{k-1}|}, \ldots, \frac{1}{|x_n^{k-1}|}, \ldots, \frac{1}{|x_N^{k-1}|}]$ is the normalization block. Thus the kth transmitted symbol of U_n's packet in Phase II is $x_n^k = u_n^k \frac{x_n^{k-1}}{|x_n^{k-1}|}$, which is differentially encoded between the combined symbol u_n^k and the $(k-1)$th symbol of the packet. The normalization block $\bar{\mathbf{D}}_x^{k-1}$ prevents the peak power of the transmitted signals from being too large or too small.

At the end of Phase II, D has received the N packets from the N user nodes. The kth signals of the received packets at D can be written as

$$\mathbf{y}^k = \sqrt{P_{II}} \mathbf{D}_x^k \mathbf{h}^k + \mathbf{w}^k, \tag{5}$$

where $\mathbf{y}^k = [y_1^k, \ldots, y_n^k, \ldots, y_N^k]^{\mathrm{T}}$, $\mathbf{w}^k = [w_1^k, \ldots, w_n^k, \ldots, w_N^k]^{\mathrm{T}} \sim \mathcal{CN}(\mathbf{0}, \mathbf{I}_N N_0)$ is the received noise vector, $\mathbf{h}^k = [h_1^k, \ldots, h_n^k, \ldots, h_N^k]^{\mathrm{T}}$ with h_n^k being the channel between U_n and D during the transmission of x_n^k. Assume that the channels do not change significantly over a period of two adjacent symbols within one packet, i.e. $h_n^k = h_n^{k-1} = h_n$ and $g_{mn}^k = g_{mn}^{k-1} = g_{mn}$. Thus we have $\mathbf{h}^k = \mathbf{h}^{k-1} = \mathbf{h}$, and the received signals can be expressed as

$$\mathbf{y}^k = \mathbf{D}_u^k \bar{\mathbf{y}}^{k-1} + \tilde{\mathbf{w}}^k, \tag{6}$$

where $\bar{\mathbf{y}}^{k-1} = \bar{\mathbf{D}}_x^{k-1} \mathbf{y}^{k-1}$ and $\tilde{\mathbf{w}}^k = \mathbf{w}^k - \mathbf{D}_u^k \bar{\mathbf{D}}_x^{k-1} \mathbf{w}^{k-1}$. The equivalent noise vector $\tilde{\mathbf{w}}^k$ is zero-mean with the covariance matrix of

$$\begin{aligned} \mathbf{\Sigma}_w &= \mathrm{E}[\tilde{\mathbf{w}}^k (\tilde{\mathbf{w}}^k)^{\mathrm{H}}] \\ &= [\mathbf{I}_N + (\bar{\mathbf{D}}_x^{k-1})^2 \mathbf{D}_u^k (\mathbf{D}_u^k)^{\mathrm{H}}] N_0 = \mathbf{\Lambda}_w N_0, \end{aligned} \tag{7}$$

where $\mathbf{\Lambda}_w = \mathrm{diag}[\varepsilon_1, \ldots, \varepsilon_n, \ldots, \varepsilon_N]$ and $\varepsilon_n = 1 + \frac{|u_n^k|^2}{|x_n^{k-1}|^2}$.

B. Signal Detection

To make the relationship clear, substitute (2) and (3) into the received signals in (6) to get

$$\mathbf{y}^k = \mathbf{SBA} \bar{\mathbf{y}}^{k-1} + \tilde{\mathbf{w}}^k, \tag{8}$$

where $\mathbf{S} = \mathrm{diag}[\mathbf{s}^{k\mathrm{T}}, \ldots, \mathbf{s}^{k\mathrm{T}}]$, $\mathbf{A} = \mathrm{diag}[\mathbf{a}_1, \ldots, \mathbf{a}_N]$, and $\mathbf{B} = \mathrm{diag}[\beta_{11}, \ldots, \beta_{N1}, \ldots, \beta_{1N}, \ldots, \beta_{NN}]$.

Based on the received signal vector in (8), the maximum likelihood (ML) detection is used at D, and the estimation of $\mathbf{s}^k$, denoted as $\tilde{\mathbf{s}}^k$, can be written as

$$\tilde{\mathbf{s}}^k = \arg \min_{\mathbf{s}^k \in \mathcal{A}^N} \{ [\mathbf{y}^k - \mathbf{SA}\bar{\mathbf{y}}^{k-1}]^{\mathrm{H}} \mathbf{\Sigma}_w^{-1} [\mathbf{y}^k - \mathbf{SA}\bar{\mathbf{y}}^{k-1}] \}. \tag{9}$$

As shown in (9), the decoding complexity of ML detection increases exponentially with the number of user nodes. Thus for large N and/or large constellation size, sphere decoding method [21] [22] can be used to reduce the complexity. For high density nodes, they can be divided into subgroups and each group uses a DSTNC of smaller size to reduce the decoding complexity while sacrificing some diversity.

As for the detection at U_n in Phase I, with the assumption that the channels do not change significantly over a period of two adjacent symbols, the received signal at U_n from U_m in Phase I becomes

$$y_{mn}^k = \sqrt{P_I} g_{mn} v_m^k + w_{mn}^k, \tag{10}$$

and the ML detection for s_m^k at U_n is

$$\hat{s}_{mn}^k = \arg \min_{s_m \in \mathcal{A}} \frac{|y_{mn}^k - s_m y_{mn}^{k-1}|^2}{\xi_m N_0}, \tag{11}$$

where $\xi_m = 1 + \frac{|s_m^k|^2}{|v_m^{k-1}|^2}$.

Note that in differential detection, because the receiver does not know the transmitted symbol, we can replace the signal terms in the variances of the equivalent noises with their means, i.e. $\varepsilon_n = 1 + \frac{E[|u_n^k|^2]}{|x_n^{k-1}|^2}$, and $\xi_m = 1 + \frac{E[|s_m^k|^2]}{|v_m^{k-1}|^2}$. Simulation results in Section V show that this approximation leads to very small performance degradation. Also note that the detection states of the user nodes are not available at D, therefore in the ML detector (9), D assumes the user nodes can successfully decode. It is shown later by the simulations that the performances with and without knowledge of the detection states at D are the same.

III. PERFORMANCE ANALYSIS AND DESIGN OF DSTNC

In this section, the performance of the DSTNC scheme is analyzed, and the PEP is derived. Based on the PEP analysis, we derive two design criteria for the network coding vectors, i.e., the diversity criterion and the product criterion.

A. PEP Analysis

The accurate performance analysis of a differential coded system requires the consideration of the quadratic receiving structure [23] [24]. We can well approximate the performance in high SNR situations by using an equivalent coherent receiver model (8) with $\bar{\mathbf{y}}^{k-1}$ acting as a known channel vector and $\tilde{\mathbf{w}}^k$ as the equivalent noise vector [25]. Since $\mathbf{\Sigma}_w$, the covariance matrix of $\tilde{\mathbf{w}}^k$, is clearly a diagonal matrix, the equivalent noise remains uncorrelated but with unequal variance entries. After normalized by $\mathbf{\Sigma}_w^{-\frac{1}{2}}$, which can be estimated at D, (8) becomes

$$\mathbf{\Sigma}_w^{-\frac{1}{2}} \mathbf{y}^k = \mathbf{\Sigma}_w^{-\frac{1}{2}} \mathbf{SBA} \bar{\mathbf{y}}^{k-1} + \bar{\mathbf{w}}^k, \tag{12}$$

where $\bar{\mathbf{w}}^k = \mathbf{\Sigma}_w^{-\frac{1}{2}} \tilde{\mathbf{w}}^k$ has a covariance matrix $N_0 \mathbf{I}_N$. The normalization just adjusts the signal strength at D so that the noise power is uniform, and it does not affect the codeword error probability.

From the above equation, we can derive the PEP, i.e. the probability of transmitting $\mathbf{s}^k$ and deciding in favor of another $\mathbf{c}^k = [c_1^k, c_2^k, \ldots, c_N^k]^{\mathrm{T}}$ at the detector, conditioned by previously received signals and the detection states at the user nodes. The PEP is given by

$$\begin{aligned} &P(\mathbf{s}^k \to \mathbf{c}^k | \bar{\mathbf{y}}^{k-1}, \{\beta_{11}, \ldots, \beta_{N1}, \ldots, \beta_{1N}, \ldots, \beta_{NN}\}) \\ &= Q\Big(\sqrt{\frac{d^2(\mathbf{S}, \mathbf{C})}{2N_0}}\Big) \le \exp\Big(-\frac{d^2(\mathbf{S}, \mathbf{C})}{4N_0}\Big), \end{aligned} \tag{13}$$

where the inequality is the Chernoff bound [26], and $d^2(\mathbf{S}, \mathbf{C})$ is the distance between the received signals corresponding to respective codeword $\mathbf{s}^k$ and $\mathbf{c}^k$. The distance can be written as

$$d^2(\mathbf{S}, \mathbf{C}) = \left(\Delta \mathbf{S} \mathbf{B} \mathbf{A} \bar{\mathbf{y}}^{k-1}\right)^{\mathrm{H}} \mathbf{\Lambda}_w^{-1} \left(\Delta \mathbf{S} \mathbf{B} \mathbf{A} \bar{\mathbf{y}}^{k-1}\right), \quad (14)$$

where $\Delta \mathbf{S} = \mathbf{S} - \mathbf{C}$ with $\mathbf{C} = \mathrm{diag}[\mathbf{c}^{k\mathrm{T}}, ..., \mathbf{c}^{k\mathrm{T}}]$. For moderate or high SNR scenarios, we make the following approximation $\mathbf{y}^{k-1} = \sqrt{P_{II}} \mathbf{D}_x^{k-1} \mathbf{h}$, and the distance becomes

$$d^2(\mathbf{S}, \mathbf{C}) = P_{II} \mathbf{h}^{\mathrm{H}} \left(\Delta \mathbf{S} \mathbf{B} \mathbf{A} \bar{\mathbf{D}}_x^{k-1} \mathbf{D}_x^{k-1}\right)^{\mathrm{H}} \mathbf{\Lambda}_w^{-1} \left(\Delta \mathbf{S} \mathbf{B} \mathbf{A} \bar{\mathbf{D}}_x^{k-1} \mathbf{D}_x^{k-1}\right) \mathbf{h}. \quad (15)$$

Assuming that channels from different nodes to D are spatially uncorrelated, averaging the bound in (13) with respect to $\mathbf{h}$ results in [26]

$$P(\mathbf{s}^k \to \mathbf{c}^k | \{\beta_{11}, \ldots, \beta_{N1}, \ldots, \beta_{1N}, \ldots, \beta_{NN}\})$$
$$\leq \mathrm{E}_{\mathbf{h}} \left[\exp\left(-\frac{d^2(\mathbf{S}, \mathbf{C})}{4N_0}\right)\right] = \prod_{n=1}^{N} \left(1 + \frac{P_{II} \lambda_n}{4N_0}\right)^{-1}, \quad (16)$$

where λ_n is the eigenvalue of the following $N \times N$ diagonal matrix

$$\mathbf{R}_h^{\frac{1}{2}} \left(\Delta \mathbf{S} \mathbf{B} \mathbf{A} \bar{\mathbf{D}}_x^{k-1} \mathbf{D}_x^{k-1}\right)^{\mathrm{H}} \mathbf{\Lambda}_w^{-1} \left(\Delta \mathbf{S} \mathbf{B} \mathbf{A} \bar{\mathbf{D}}_x^{k-1} \mathbf{D}_x^{k-1}\right) \mathbf{R}_h^{\frac{1}{2}} \quad (17)$$

with $\mathbf{R}_h = \mathrm{diag}[\sigma_1^2, \ldots, \sigma_N^2]$ being the correlation matrix of $\mathbf{h}$. It is easy to verify that the nth eigenvalue is $\lambda_n = \frac{\sigma_n^2}{\varepsilon_n} |\sum_{m=1}^{N} \beta_{mn} a_{mn} \Delta s_m|^2$ with $\Delta s_m = s_m^k - c_m^k$.

Averaging with respect to the detection states of the user nodes, the PEP can be written as

$$P(\mathbf{s}^k \to \mathbf{c}^k) \leq \mathrm{E}_{\beta_{mn}} \left[\prod_{n=1}^{N} \left(1 + \frac{P_{II} \lambda_n}{4N_0}\right)^{-1}\right]. \quad (18)$$

Because the signal detection at each user is independent and the detection of symbols from different sources at a certain user is also independent, the order of expectation operator and production operator in (18) can be exchanged as follows

$$P(\mathbf{s}^k \to \mathbf{c}^k) \leq \prod_{n=1}^{N} \mathrm{E}_{\beta_{mn}} \left[\left(1 + \frac{P_{II} \sigma_n^2 |\sum_{m=1}^{N} \beta_{mn} a_{mn} \Delta s_m|^2}{4N_0 \varepsilon_m}\right)^{-1}\right]. \quad (19)$$

Assuming that the SER at U_n for the symbols from U_m is p_{mn}, β_{mn}'s are independent Bernoulli random variables with a distribution

$$P(\beta_{mn}) = \begin{cases} 1 - p_{mn}, & \text{for } \beta_{mn} = 1 \\ p_{mn}, & \text{for } \beta_{mn} = 0. \end{cases} \quad (20)$$

Considering all possibilities of the detection state $\{\beta_{11}, \ldots, \beta_{N1}, \ldots, \beta_{1N}, \ldots, \beta_{NN}\}$, the PEP can be written as (21) which is shown on the top of this page. The first term in (21) represents the case when all symbols received at U_n are decoded correctly, the second term represents the case when one of the symbols received at U_n is decoded incorrectly, and so on. When SNR is high, SERs are small and the higher order terms of SERs could be ignored. Thus the PEP can be approximated by (22) on the top of this page, where H.O.T. stands for the higher order terms.

Diversity is an important criterion since it determines the slop of the performance curve. However, it is obvious from (22) that $|\mathbf{a}_n^{\mathrm{T}} \Delta \mathbf{s}| = 0$ would result in the loss of diversity. In order to achieve the maximum diversity, the first criterion of the network coding vectors is derived as follows.

Diversity criterion: The full diversity gain N can be achieved if the following maximum diversity condition holds true for any distinct pair $\{\mathbf{s}^k, \mathbf{c}^k\}$,

$$|\mathbf{a}_n^{\mathrm{T}} \Delta \mathbf{s}| \neq 0, \quad \forall n \in [1, N], \forall \mathbf{s}^k, \mathbf{c}^k \in \mathcal{A}^N. \quad (23)$$

Theorem 1: Let d_{max} represent the maximum Euclidean distance of $\mathcal{A}$. If $\forall n \in [1, N]$, $|\mathbf{a}_n^{\mathrm{T}} \Delta \mathbf{s}| \neq 0$ holds true for any distinct pair $\{\mathbf{s}^k, \mathbf{c}^k\}$, the PEP under high SNR is upper bounded by

$$P(\mathbf{s}^k \to \mathbf{c}^k) < G\left(\frac{P_t}{N_0}\right)^{-N} \quad (24)$$

where G is coding advantage and

$$G = \prod_{n=1}^{N} \frac{1}{|\mathbf{a}_n^{\mathrm{T}} \Delta \mathbf{s}|^2} \left(\frac{4\varepsilon_n}{(1-\alpha)\sigma_n^2} + \sum_{l=1, l \neq n}^{N} \frac{N C_M \xi_l d_{max}^2}{\alpha \sigma_{ln}^2}\right)$$

with $\alpha = \frac{P_I}{P_t}$. C_M is constant for a certain constellation.
Proof: See Appendix.

It can be seen from (24) that, for a fixed number of user nodes, the adopted signal constellation, the power allocation α and channel conditions can influence the coding advantage G but not the diversity order. When given the constellation, α and channel conditions, the PEP depends on the design of network coding vectors. Thus according to Theorem 1, the second design criterion is derived as follows to get a better performance.

Product criterion: The minimum value of the product $\prod_{n=1}^{N} |\mathbf{a}_n^{\mathrm{T}} \Delta \mathbf{s}|^2$ over all pairs of distinct signal vectors $\mathbf{s}^k$ and $\mathbf{c}^k$ should be as large as possible.

The product criterion is of secondary importance and should be optimized if full diversity is achieved.

B. Design of DSTNC

Let $\mathbf{A}_N$ denote the combining matrix (network coding matrix), which is constructed from the network coding vectors of the N user nodes as follows

$$\mathbf{A}_N^{\mathrm{T}} = [\mathbf{a}_1 \cdots \mathbf{a}_n \cdots \mathbf{a}_N]. \quad (25)$$

Let $\mathbf{s}_f = \mathbf{A}_N \mathbf{s}$, where $\mathbf{s} = [s_1, \ldots, s_N]^{\mathrm{T}} \in \mathcal{A}^N$. According to the diversity criterion, $\mathbf{A}_N$ should be designed to satisfy the following property: the original signal constellation is rotated and expanded such that there is no zero entry in the vector $\mathbf{s}_f$ for any $\mathbf{s} \neq \mathbf{0}_N$. This is referred to as the signal space diversity technique [27] [28]. According to the product criterion, the minimum product distance of a set of signal points should be maximized, which is also investigated in [27], [28]. This diversity technique has been applied to MIMO coding schemes such as [29], [30]. Note that the combining matrices can be constructed based on Hadamard matrices and Vandermonde matrices. However, the combing matrices based on Vandermonde matrices result in larger minimum product distance than those based on Hadamard matrices [30]. A combining matrix based on Vandermonde matrices with parameters $\theta_1, \theta_2, \ldots, \theta_N$ can be written as

$$P(\mathbf{s}^k \rightarrow \mathbf{c}^k) \leq \prod_{n=1}^{N} \Big[\frac{1}{1 + \frac{P_{II}\sigma_n^2}{4N_0\varepsilon_n}|\mathbf{a}_n^{\mathrm{T}}\Delta\mathbf{s}|^2} \prod_{m=1,m\neq n}^{N} (1 - p_{mn})$$

$$+ \sum_{l=1,l\neq n}^{N} \Big(\frac{1}{1 + \frac{P_{II}\sigma_n^2}{4N_0\varepsilon_n}|\sum_{m=1,m\neq l}^{N} a_{mn}\Delta s_m|^2} \prod_{i=1,i\neq l,i\neq n}^{N} (1 - p_{in})p_{ln} \Big) + \cdots + \frac{1}{1 + \frac{P_{II}\sigma_n^2}{4N_0\varepsilon_n}|a_{nn}\Delta s_n|^2} \prod_{m=1,m\neq n}^{N} p_{mn} \Big], \tag{21}$$

$$P(\mathbf{s}^k \rightarrow \mathbf{c}^k) \leq \prod_{n=1}^{N} \Big[\frac{1}{1 + \frac{P_{II}\sigma_n^2}{4N_0\varepsilon_n}|\mathbf{a}_n^{\mathrm{T}}\Delta\mathbf{s}|^2}(1 - \sum_{m=1,m\neq n}^{N} p_{mn}) + \sum_{l=1,l\neq n}^{N} \frac{1}{1 + \frac{P_{II}\sigma_n^2}{4N_0\varepsilon_n}|\sum_{m=1,m\neq l}^{N} a_{mn}\Delta s_m|^2}p_{ln} + \text{H.O.T.} \Big]$$

$$\leq \prod_{n=1}^{N} \Big[\frac{1}{1 + \frac{P_{II}\sigma_n^2}{4N_0\varepsilon_n}|\mathbf{a}_n^{\mathrm{T}}\Delta\mathbf{s}|^2}(1 - \sum_{m=1,m\neq n}^{N} p_{mn}) + \sum_{l=1,l\neq n}^{N} p_{ln} + \text{H.O.T.} \Big], \tag{22}$$
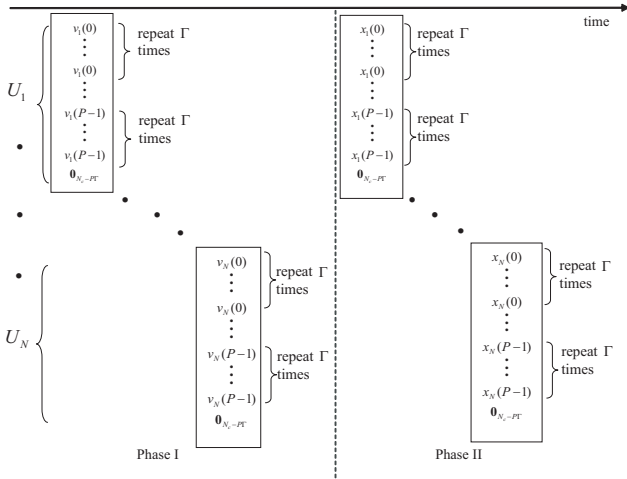

Fig. 4. The construction of DSTFNC for broadband cooperative communications.

$$\mathbf{A}_N^{\mathrm{T}}(\theta_1, \theta_2, \ldots, \theta_N) = \frac{1}{\sqrt{N}} \begin{bmatrix} 1 & 1 & \cdots & 1 \\ \theta_1 & \theta_2 & \cdots & \theta_N \\ \vdots & \vdots & \ddots & \vdots \\ \theta_1^{N-1} & \theta_2^{N-1} & \cdots & \theta_N^{N-1} \end{bmatrix}. \tag{26}$$

Some best known transform matrices $\mathbf{A}_N^{\mathrm{T}}$ based on Vandermonde matrices are summarized in [30]. More constructions and details of the transform matrices can be found in [27], [28].

Based on the above description, the network coding vector for U_n is

$$\mathbf{a}_n = \frac{1}{\sqrt{N}}[1 \ \theta_n \ \cdots \ \theta_n^{N-1}]^{\mathrm{T}}, \tag{27}$$

where θ_n is determined by the number of nodes and the construction method. This means each node can independently generate its combining function according to the assigned parameter $\theta_n, n \in [1, N]$. With these network coding vectors, the proposed DSTNC scheme can achieve full diversity, which equals the number of user nodes, without the requirement of synchronization or channel estimation.

IV. DESIGN OF DSTFNC FROM DSTNC

In this section we consider the differential transmission for broadband multi-source cooperative communications. The

channels in the network shown in Fig. 2 are assumed frequency selective fading. Assume that the numbers of multipaths between any pair of user nodes and between the user nodes and D are L_1 and L_2, respectively. The channel frequency response from U_m to U_n is given by $G_{mn}(q) = \sum_{l=0}^{L_1-1} g_{mn}(l)e^{-j\frac{2\pi q\tau_{mn}(l)}{T}}$, where $q \in [0, N_c-1]$, $g_{mn}(l)$ and $\tau_{mn}(l)$ are the complex amplitude and delay of the lth path, respectively, and T is the OFDM symbol period. The channel coefficients $g_{mn}(l)$'s are modeled as zero-mean complex Gaussian variables with variances $\mathrm{E}|g_{mn}(l)|^2 = \sigma_{mn,l}^2$. $g_{mn}(l)$ for different $m, n \in [1, N]$ and $l \in [0, L_1-1]$ are assumed independent, and the total power is $\sum_{l=0}^{L_1-1} \sigma_{mn,l}^2 = \sigma_{mn}^2$. The channel frequency response from U_m to D is given by $H_m(q) = \sum_{l=0}^{L_2-1} h_m(l)e^{-j\frac{2\pi q\tau_m(l)}{T}}$, where $h_m(l)$ and $\tau_m(l)$ are the complex amplitude and delay of the lth path, respectively. The channel coefficients $h_m(l)$'s are modeled as zero-mean complex Gaussian variables with variances $\mathrm{E}|h_m(l)|^2 = \sigma_{m,l}$ and $h_m(l)$ for different $m \in [1, N]$ and $l \in [0, L_2-1]$ are assumed independent. The total power is normalized such that $\sum_{l=0}^{L_2-1} \sigma_{m,l}^2 = \sigma_m^2$. TDMA is still used in Phase I and Phase II to overcome the imperfect synchronization issue. Each user node employs an OFDM modulator with N_c subcarriers. Based on the proposed DSTNC scheme, a differential encoding scheme in frequency domain within each OFDM block is designed.

A. Distributed DSTFNC From DSTNC

The distributed DSTFNC scheme is motivated by the differential space-frequency modulation scheme in [20]. Full diversity space frequency codes for MIMO-OFDM systems are obtained from space time codes via mapping in [31]. In this subsection, we will generate the DSTFNC for broadband multi-source cooperative communication systems by mapping from the proposed DSTNC.

The two phases of a transmission is illustrated in Fig. 4, which has a similar structure to Fig. 3. The OFDM block for each user is divided into P groups in which each transmitted symbol is repeated Γ times, where $1 \leq \Gamma \leq L_2$ and $P = \lfloor \frac{N_c}{\Gamma} \rfloor$, i.e., the largest integer not greater than $\frac{N_c}{\Gamma}$. The integer Γ is adjustable for different diversities. $p = 0$ is the reference group for the differential coding.

1) Differential Transmission in Phase I: The pth group in the mth OFDM period received at U_n in Phase I can be written

as

$$\mathbf{y}_{mn}^p = \sqrt{P_I}\mathbf{1}_\Gamma \otimes v_m(p)\mathbf{G}_{mn}^p + \mathbf{w}_{mn}^p, \qquad (28)$$

where $\mathbf{y}_{mn}^p = [y_{mn}(k_{p,1}),...,y_{mn}(k_{p,\Gamma})]^T$ with $y_{mn}(k_{p,l})$ being the signal received from U_m on the $k_{p,l}$th subcarrier, and $\mathbf{w}_{mn}^p = [w_{mn}(k_{p,1}),...,w_{mn}(k_{p,\Gamma})]^T$ with $w_{mn}(k_{p,\gamma})$ being the zero-mean and N_0-variance AWGN on the k_{pl}th subcarrier received from U_m at U_n, and $\mathbf{G}_{mn}^p = [G_{mn}(k_{p,1}),...,G_{mn}(k_{p,\Gamma})]^T$. As in Section II. A, the transmitted symbol is $v_m(p) = s_m(p)\frac{v_m(p-1)}{|v_m(p-1)|}$, where $s_m(p)$ is the pth information symbol of U_m. Note that the processing is the same as that for frequency flat fading except that the differential modulation is performed over subcarriers.

After decoding in Phase I, U_n obtains a set of estimations $\hat{\mathbf{S}}_n = [\hat{\mathbf{s}}_{1n},....,\hat{\mathbf{s}}_{mn},...,\hat{\mathbf{s}}_{Nn}]^T$ from other users, where $\hat{\mathbf{s}}_{mn} = [\hat{s}_{mn}(0),\hat{s}_{mn}(1),...,\hat{s}_{mn}(P-1)]^T$ is the estimated signal vector from U_m. According to (3), the combined symbol generated at U_n for $p = 0,1,..P-1$ is

$$u_n(p) = f_n(\hat{\mathbf{s}}_n(p)) = \sum_{m=1}^N a_{mn}\hat{s}_{mn}(p) = \mathbf{a}_n^T\hat{\mathbf{s}}_{n,p}, \qquad (29)$$

where $\hat{\mathbf{s}}_{n,p} = [\hat{s}_{1n}(p),\hat{s}_{2n}(p),...,\hat{s}_{Nn}(p)]^T$ and $\mathbf{a}_n$ is the coding vector designed in Section III.

2) Differential Transmission in Phase II: Because D does not have any kind of CSI, the users transmit their pth combined symbols $\mathbf{u}_p = [u_1(p),u_2(p),...,u_N(p)]$ differentially. Let $\mathbf{X}_p$ denote the pth group of the DSTFNC, which can be formulated as

$$\mathbf{X}_p = \mathbf{1}_\Gamma \otimes \mathbf{D}_x^p, \qquad (30)$$

where $\mathbf{D}_x^p = \mathrm{diag}[x_1(p),x_2(p),...,x_N(p)]$ with $x_n(p)$ being the transmitted symbol in the pth group of the OFDM symbol from U_n. $\mathbf{D}_x^p$ is differentially encoded according to (4),

$$\mathbf{D}_x^p = \mathbf{D}_u^p\mathbf{D}_x^{p-1}\bar{\mathbf{D}}_x^{p-1}, \qquad (31)$$

where $\mathbf{D}_u^p = \mathrm{diag}[u_1(p),u_2(p),...,u_N(p)]$, $\mathbf{D}_x^{p-1} = \mathrm{diag}[x_1(p-1),x_2(p-1),...,x_N(p-1)]$, and $\bar{\mathbf{D}}_x^{p-1} = \mathrm{diag}[\frac{1}{|x_1(p-1)|},\frac{1}{|x_2(p-1)|},...,\frac{1}{|x_N(p-1)|}]$. Obviously, $\mathbf{D}_x^p$ is the DSTNC in Section II. The difference is that the DSTNC is differentially encoded in time domain while the DSTFNC is in frequency domain. Ignoring the zeros filled in Fig. 4(b) when N_c is not an integer multiple of $N\Gamma$, the DSTFNC can be written as a concatenation of the P groups

$$\mathbf{X} = [\mathbf{X}_0^T,\mathbf{X}_1^T,...,\mathbf{X}_{P-1}^T]^T. \qquad (32)$$

Let $\mathbf{D}_{X_p} = \mathrm{diag}[x_1(p),\ldots,x_N(p),\ldots,x_1(p),\ldots,x_N(p)]$ denote the diagonal version of $\mathbf{X}_p$. Then the pth group of the received signals at D can be written as

$$\mathbf{y}^p = \sqrt{P_{II}}\mathbf{D}_{X_p}\mathbf{H}^p + \mathbf{w}^p, \qquad (33)$$

where $\mathbf{H}^p = [H_1(k_{p,1}^{(1)}),\ldots,H_N(k_{p,1}^{(N)}),\ldots,H_1(k_{p,\Gamma}^{(1)}),\ldots,H_N(k_{p,\Gamma}^{(N)})]^T$ is the pth group of channel vector with $k_{p,\gamma}^{(m)} \in [0,N_c-1]$ being the index of subcarrier on which $x_m(p)$ is transmitted by U_m, $\mathbf{y}^p = [y_1(k_{p,1}^{(1)}),\ldots,y_N(k_{p,1}^{(N)}),\ldots,y_1(k_{p,\Gamma}^{(1)}),\ldots,y_N(k_{p,\Gamma}^{(N)})]^T$ is the pth group of the received signal vector with $y_m(k_{p,\gamma}^{(m)})$ being the signal received from U_m on the $k_{p,\gamma}^{(m)}$th subcarrier, and $\mathbf{w}^p = [w_1(k_{p,1}^{(1)}),\ldots,w_N(k_{p,1}^{(N)}),\ldots,w_1(k_{p,\Gamma}^{(1)}),\ldots,w_N(k_{p,\Gamma}^{(N)})]^T$ with $w_m(k_{p,\gamma}^{(m)})$ being the zero-mean AWGN with variance N_0

received by D on the $k_{p,\gamma}^{(m)}$th subcarrier during the mth OFDM period in Phase II. It can be seen from (30)-(32) that the signals are differentially encoded over groups of subcarriers. Define $\boldsymbol{\Delta}_{h,p} = \mathbf{H}_p - \mathbf{H}_{p-1}$ as the channel difference between $\mathbf{H}_p$ and $\mathbf{H}_{p-1}$. Since $\mathbf{y}^p = \sqrt{P_{II}}\mathbf{D}_{X_p}\mathbf{H}^p + \mathbf{w}^p$ and $\mathbf{D}_{X_p} = \mathbf{I}_\Gamma \otimes (\mathbf{D}_u^p\bar{\mathbf{D}}_x^{p-1})\mathbf{D}_{X_{p-1}}$, we have

$$\mathbf{y}^p = \mathbf{I}_\Gamma \otimes (\mathbf{D}_u^p\bar{\mathbf{D}}_x^{p-1})\mathbf{y}^{p-1} + \sqrt{P_{II}}\mathbf{D}_{X_p}\boldsymbol{\Delta}_{h,p} + \tilde{\mathbf{w}}^p \quad (34)$$

where $\tilde{\mathbf{w}}^p = \mathbf{w}^p - \mathbf{I}_\Gamma \otimes (\mathbf{D}_u^p\bar{\mathbf{D}}_x^{p-1})\mathbf{w}^{p-1}$. The equivalent noise $\tilde{\mathbf{w}}^p$ is zero-mean and the variance is

$$\begin{aligned}\boldsymbol{\Sigma}_w' &= \mathrm{E}[\tilde{\mathbf{w}}^p(\tilde{\mathbf{w}}^p)^H] \\ &= \mathbf{I}_\Gamma \otimes [\mathbf{I}_N + (\bar{\mathbf{D}}_x^{p-1})^2\mathbf{D}_u^p(\mathbf{D}_u^p)^H]N_0 = \boldsymbol{\Lambda}_w'N_0.\end{aligned} \qquad (35)$$

It is obvious that $\boldsymbol{\Lambda}_w' = \mathbf{I}_\Gamma \otimes \boldsymbol{\Lambda}_w$, where $\boldsymbol{\Lambda}_w$ is defined in (7).

B. Decoding and Channel Permutation

1) Decoding at D in Phase II: We consider differential decoding over two adjacent received groups $\mathbf{y}^p$ and $\mathbf{y}^{p-1}$ for any $p = 1,2,...P-1$, where $p = 0$ is the reference group. Let $\mathbf{s}_p = [s_1(p),s_2(p),...,s_N(p)]^T$ denote the pth information symbols from the N user nodes and $\mathbf{S} = \mathrm{diag}[\mathbf{s}_p^T,...,\mathbf{s}_p^T]$. If $\mathbf{H}^p \approx \mathbf{H}^{p-1}$, or $\|\boldsymbol{\Delta}_{h,p}\|_F$ is small enough such that $\sqrt{P_{II}}\|\boldsymbol{\Delta}_{h,p}\|_F$ is much less than $\|\tilde{\mathbf{w}}_p\|_F$ [20], then a near ML decoding can be performed as (36) on the top of this page. When N and/or constellation size is large, sphere decoder [21] [22] can be used to reduce the decoding complexity.

2) Channel Permutation at Each User Node in Phase II: When the delay spread is small with respect to the OFDM period, the channel frequency response changes slowly over two adjacent subcarriers. In this case, the subcarrier indices $k_{p,\gamma}^{(m)}$ and $k_{p-1,\gamma}^{(m)}$ for U_m, $m \in [1,N]$, can be chosen as the two adjacent subcarriers of $\mathbf{H}_m = [H_m(0),H_m(1),...,H_m(N_c-1)]$. When the delay spread is large with respect to the OFDM period, the channel frequency response changes rapidly. In this case, when the statistical channel PDP (not exact CSI) from U_n to D is known at U_n, we can permute the subcarriers to get smooth logical channels so that the differential decoding can be performed successfully. Because the permutation optimization by maximizing the SER or bit error rate (BER) is intractable, we consider an permutation approach of maximizing the average SNR as in [20].

Define the average SNR as

$$\mathrm{SNR}_{av} = \frac{\sum_{p=1}^{P-1}\left(\mathrm{E}\|\mathbf{I}_\Gamma \otimes (\mathbf{D}_u^p\bar{\mathbf{D}}_x^{p-1})\mathbf{y}^{p-1}\|_F^2\right)}{\sum_{p=1}^{P-1}\left(\mathrm{E}\|\sqrt{P_{II}}\mathbf{D}_{X_p}.\boldsymbol{\Delta}_{h,p} + \tilde{\mathbf{w}}^p\|_F^2\right)}. \qquad (37)$$

We try to minimize $\sum_{p=1}^{P-1}\left(\mathrm{E}\|\sqrt{P_{II}}\mathbf{D}_{X_p}\boldsymbol{\Delta}_{h,p} + \tilde{\mathbf{w}}^p\|_F^2\right)$ to maximize SNR_{av}. Because the noise, the signals, and the channels are independent with each other, we can simplify the minimization problem as (38) on the top of this page, where $\Phi_n = \sum_{p=1}^{P-1}\left(\mathrm{E}|x_n(p)|^2\mathrm{E}\sum_{\gamma=1}^\Gamma |H_n(k_{p,\gamma}^{(n)}) - H_n(k_{p-1,\gamma}^{(n)})|^2\right)$. $\mathrm{E}|x_n(p)|^2$ is a constant related to the signal constellation, so we will omit it in the following. It can be seen from (38) that the minimization problem can be solved by minimizing Φ_n independently at each user node. Therefore, the permutation approach for a certain user node U_n is considered and the other nodes can permute their subcarriers in the same way.

$$\tilde{\mathbf{s}}_p = \arg \min_{\mathbf{s}_p \in \mathcal{A}^N} \{ [\mathbf{y}^p - \mathbf{I}_\Gamma \otimes (\mathbf{SA\bar{D}}_x^{p-1})\mathbf{y}^{p-1}]^\mathrm{H} (\mathbf{\Sigma}_w')^{-1} [\mathbf{y}^p - \mathbf{I}_\Gamma \otimes (\mathbf{SA\bar{D}}_x^{p-1})\mathbf{y}^{p-1}] \}. \tag{36}$$

$$\min \sum_{p=1}^{P-1} \left(\mathrm{E} \| \sqrt{P_{II}} \mathbf{D}_{X_p} \mathbf{\Delta}_{h,p} \|_\mathrm{F}^2 \right) = \min \sum_{p=1}^{P-1} \left(P_{II} \sum_{n=1}^{N} (\mathrm{E}|x_n(p)|^2 \mathrm{E} \sum_{\gamma=1}^{\Gamma} |H_n(k_{p,\gamma}^{(n)}) - H_n(k_{p-1,\gamma}^{(n)})|^2) \right)$$

$$= \min P_{II} \sum_{n=1}^{N} \Phi_n, \tag{38}$$

$$\Phi_n = \mathrm{E} \sum_{p=1}^{P-1} \sum_{\gamma=1}^{\Gamma} \sum_{l=0}^{L_2-1} | \sum_{l=0}^{L_2-1} h_n(l) e^{-j \frac{2\pi k_{p,\gamma}^{(n)} \tau_n(l)}{T}} - \sum_{l=0}^{L_2-1} h_n(l) e^{-j \frac{2\pi k_{p-1,\gamma}^{(n)} \tau_n(l)}{T}} |^2$$

$$= \sum_{p=1}^{P-1} \sum_{\gamma=1}^{\Gamma} \sum_{l=0}^{L_2-1} 4\sigma_{n,l}^2 \sin^2 [\frac{\tau_n(l)(k_{p,\gamma}^{(n)} - k_{p-1,\gamma}^{(n)})}{T}]. \tag{39}$$

For U_n, Φ_n can be written as (39), which is on the top of this page. Let $d(i,j) = \sum_{l=0}^{L_2-1} 4\sigma_{n,l}^2 \sin^2 [\frac{\tau_n(l)(i-j)}{T}]$. Then Φ_n becomes

$$\Phi_n = \sum_{p=1}^{P-1} \sum_{\gamma=1}^{\Gamma} d(k_{p,\gamma}^{(n)}, k_{p-1,\gamma}^{(n)}). \tag{40}$$

The minimization of Φ_n in (40) is the shortest-path problem [32] and can be solved by using the idea of Dijkstra's algorithm [20], [32] as follows.

- Let $V_0 = \{1, 2, ..., P\Gamma\}$. Randomly choose Γ elements $\{k_{0,1}, ..., k_{0,\Gamma}\}$ from V_0 to form a set E_0, and let the rest elements be $V_1 = V_0 - E_0$.
- For p=1:P-1
  1) Choose Γ elements $\{k_{p,1}, ..., k_{p,\Gamma}\}$ from V_p to form a set E_p whose elements are nearest to the set E_{p-1}, i.e., to minimize $\sum_{\gamma=1}^{\Gamma} d(k_{p,\gamma}, k_{p-1,\gamma})$.
  2) Denote the set of the rest elements as $V_{p+1} = V_p - E_p$.

By independently minimizing Φ_n, $n \in [1, N]$, each user can get a smooth logical channel.

3) Decoding and Channel Permutation in Phase I: As for the signal detection in Phase I, differential decoding is performed. Define $\mathbf{\Delta}_{g,p} = \mathbf{G}_{mn}^p - \mathbf{G}_{mn}^{p-1}$ as the channel difference between $\mathbf{G}_{mn}^p$ and $\mathbf{G}_{mn}^{p-1}$. Assuming that $\mathbf{G}_{mn}^p \approx \mathbf{G}_{mn}^{p-1}$, or $\|\mathbf{\Delta}_{g,p}\|_\mathrm{F}$ is small enough, a near ML detection for $s_m(p)$, $p \in [0, P-1]$, can be written as

$$\hat{s}_{mn}(p) = \arg \min_{s_m \in \mathcal{A}} \sum_{\gamma=1}^{\Gamma} \frac{|y_{mn}^p(k_{p,\gamma}) - s_m y_{mn,p-1}(k_{p-1,\gamma})|^2}{\xi_m' N_0}, \tag{41}$$

where $\xi_m' = 1 + \frac{\mathrm{E}|s_m(p)|^2}{|v_m(p-1)|^2}$. To decode successfully for different delay spreads, the sets of the subcarriers can be permutated through the same way described above.

V. SIMULATION RESULTS

In this section, we present simulation results of the DSTNC and the STFNC for narrow-band and broadband wireless multi-source cooperative communications, respectively. Various numbers of user nodes are used with N= 2, 3, and 4. The corresponding network coding vectors are generated
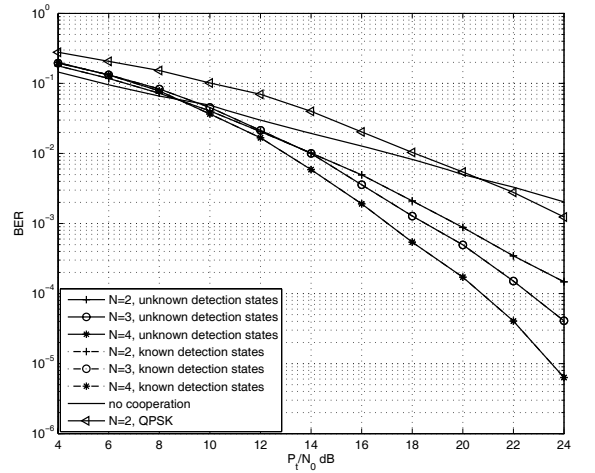

Fig. 5.   BER performance of DSTNC for different number of user nodes with $d_u = d/3$.

according to (27). For $N = 2$, $\theta_n = e^{j \frac{4n-3}{4} \pi}$ with $n = 1, 2$, for $N = 3$, $\theta_n = e^{j(\frac{1}{9} + \frac{2(n-1)}{3})\pi}$ with $n = 1, 2, 3$, and for $N = 4$, $\theta_n = e^{j \frac{4n-3}{8} \pi}$ with $n = 1, 2, 3, 4$. In the simulations, the user nodes have the same distance from D, denoted by d, and the channel variance between the user nodes to D is assumed to be 1. The inter-user distances are the same and denoted by d_u with $d_u < d$. The path loss exponent is $\nu = 3$. The total transmit power of each user for one transmission is $P_t = P_I + P_{II}$, and $P_I = \alpha P_t$. In this work, we do not derive the optimal value for α because solving the optimization problem requires CSI of all the links known at each user node or a central controller. Such an optimization problem is out of the scope of this paper. However, the influence of α on the performance of the proposed schemes is given in the simulations. For the narrow-band cooperative communications, the channel coefficients follow the Jakes' model [33] with Doppler frequency f_D and normalized fading parameter $f_D T_s$, where T_s is the sampling period which equals the symbol period. Unless specified otherwise, $f_d T_s = 0.0025$ is used throughout the simulation.
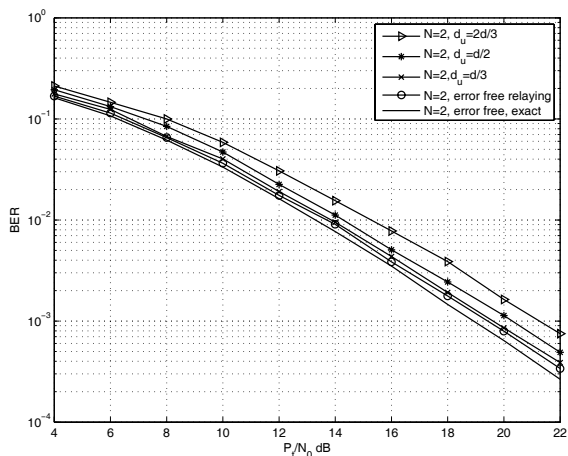
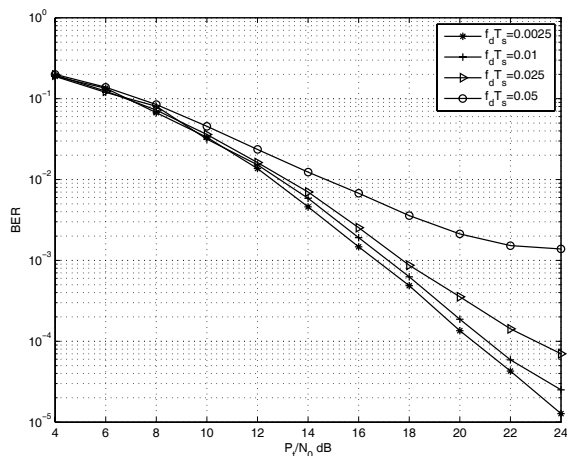Fig. 6.   BER performance of DSTNC for different distance between the user nodes with $N = 2$.

Fig. 8.   BER performance of DSTNC for different Doppler frequency with $N = 4$.
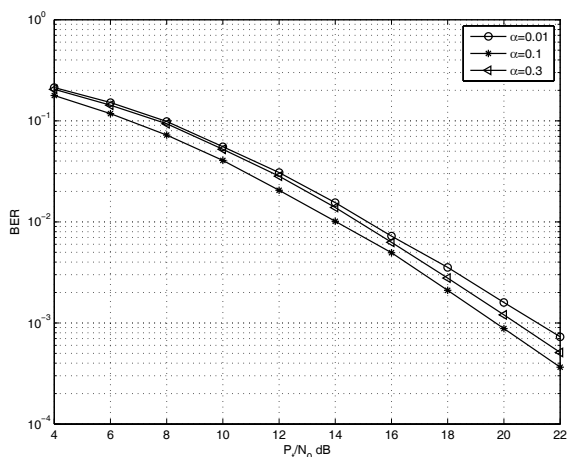

Fig. 7.   The influence of different α on BER performance of DSTNC with $N = 2$.

Fig. 5 shows the BER performance versus SNR P_t/N_0 of the DSTNC scheme with $N = 2, 3, 4$ user nodes. In the simulation, $\alpha = 0.1$, $d_u = d/3$ and BPSK is adopted. From the dashed and solid curves, we can see that the BER performances for a certain number of user nodes are the same no matter the detection states of the user nodes are known at D or not. From the curves, we verify that the full diversity order, which is equal to the number of user nodes N, is achieved by the proposed DSTNC scheme. The single node scenario without cooperation is also considered for a comparison. The user node without cooperation transmits the same symbol with the same power P_t. It can be seen clearly from Fig. 5 that the BER performance of single node without cooperation is improved by user cooperation, and the improvement becomes more significant as the number of cooperation nodes increases, due to the increase in diversity order. When SNR is low, the cooperative transmissions show no performance advantage. This is because the user nodes do not relay most of the received symbols due to the high BER. To compare with the same transmit bit rate, we also

give the BER curve for $N = 2$ users with QPSK. We can see that the BER performance with QPSK is worse than that with BPSK due to the smaller coding advantage of QPSK. But the cooperative transmission with QPSK outperforms the non-cooperative transmission when SNR is high enough because of higher diversity order. For BER of practical interest, which is usually better than 10^{-3}, cooperative transmission is better than non-cooperative transmission with the same transmission rate.

Fig. 6 depicts the BER performances for different inter-user distances with $N = 2$ and $\alpha = 0.1$. It can be seen from Fig. 6 that, as the inter-user distance d_u decreases, the BER performance becomes better. When the inter-user distance is one third of the distance between the user nodes and the destination, the performance of the proposed scheme with BPSK modulation is almost the same as that of the error-free relaying case. This performance is similar to that of a MISO system with N transmit antennas. Compared to the error-free relaying case, the performance degradation increases as d_u comes close to d. These observations match the analysis in Section III. From Theorem 1 we can see that the PEP is influenced by the inter-user distance through $\sigma_{ln}^2 \propto d_{ln}^{-\alpha}$. Therefore, when the nodes are closer to each other, the channel variance becomes larger and better performance can be achieved. In many practical situations with adjacent cooperative nodes, the proposed DSTNC scheme can obtain a performance similar to the MISO system while overcoming some practical issues in cooperative communications. In the differential detection of (9) and (11), the signal terms in ε_m and ξ_m are replaced by their mean values 1. To show the effect of this substitution, the BER performance of the ideal case which is error-free relaying and uses exact values of the symbols in detection is also plotted in Fig. 6. From the solid curve and the curve with circles we can see that, compared to the ideal case, the BER performance with mean value is slightly worse.

Fig. 7 shows the influence of α on the BER performance of the proposed DSTNC scheme. In the simulation, $N = 2$ users. BPSK is used for the proposed DSTNC scheme. First

TABLE I
NOKIA ROOFTOP CHANNEL 10-RAY POWER DELAY PROFILE

Delay profile (μs)	0	0.03	0.07	0.11	0.15	0.19	0.23	0.27	0.31	0.35
Power Profile	0.7094	0.1782	0.0577	0.0310	0.0126	0.0060	0.0028	0.0011	0.0009	0.0004
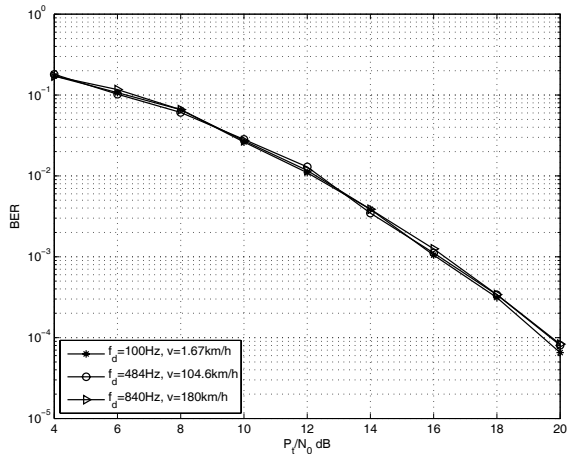
Fig. 9. BER performance of DSTFNC for different Doppler frequency with $N = 2$.

Fig. 10. BER performance of DSTFNC with different achievable diversity for different Γ and channel permutation, $N = 2$.

we can see that different value of α does not affect the slope of the performance curve but only shifts it. In order words, the diversity order is invariant with α while the coding advantage depends on it, as discussed in Section III.A. Since the total power P_t is fixed, larger α can get better BER performance at the user nodes, but degrade the relaying performance in Phase II. Smaller α means lager transmit power for Phase II, but the BER in Phase I becomes higher, which may influence the overall performance.

Fig. 8 presents the BER performance of the DSTNC scheme for different Doppler frequencies. Assume that $N = 4$, $d_u = d/3$, $\alpha = 0.1$ and BPSK modulation is used. Because the differential scheme requires the channels do not change significantly during a period of two adjacent symbols, the performance degrades as the Doppler frequency increases, associated with decreasing channel coherence time. We can see from Fig. 8 that the performance degradation is quite small when $f_d T_s$ increases to 0.01, but error floors appear when $f_d T_s \geq 0.025$. Although the performance of DSTNC degrades when the channel changes rapidly, it still can work in some situations where coherent detection is impractical. For example, considering a vehicle transmitting at a symbol rate of 30 kHz and a frequency of 1.9 GHz. When $f_d T_s = 0.025$, the vehicle moves at about 426km/h, which is approaching the required speed for trains in third-generation European cellular standards [23], and the coherence time is on the order of 20 symbols. If five training symbols were used per antenna pair [23], a cooperative communication system with $N = 4$ users would require about 20 training symbols for the channel estimations, which is a 100% overhead.

The BER performances of the DSTFNC scheme for broadband cooperative communications are given in Fig. 9 and Fig. 10. The DSTFNC is mapped from the DSTNC used in
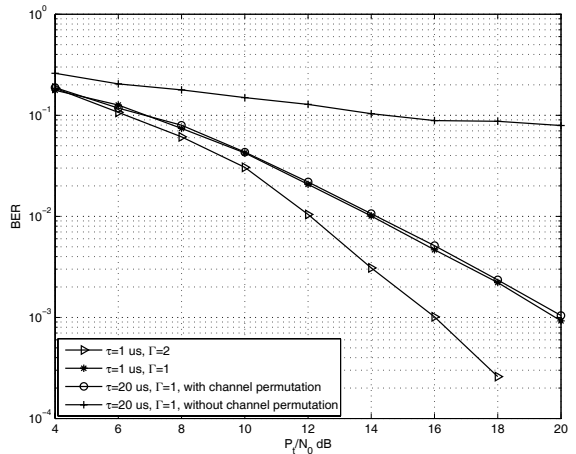
the previous simulations. There are $N = 2$ user nodes in the cooperative system and $\alpha = 0.1$.

The influence of Doppler effects is investigated in Fig. 9. In this simulation, non-line of sight (NLOS) Nokia rooftop wideband channel model in a suburban environment [34] is used. Table I shows a 10-tap delay line model to model its average power-delay profile. Each OFDM modulator has $N_c = 64$ subcarriers with the total bandwidth of 20MHz and works in $5GHz$ band. The OFDM symbol duration is $3.2\mu s$ and the length of cyclic prefix is $0.8\mu s$. Different Doppler effects caused by different speeds are considered in Fig. 9. For walking speed $v = 1.67km/h$ $(6m/s)$, the Doppler frequency offset f_d is so small that the channel can be regarded as unchanged in one OFDM block. As speed increases, Doppler effect becomes more severe. However, as can be seen from Fig. 9, the BER performances of the DSTFNC scheme with $v = 104.6km/h$ and $180km/h$ are similar to that with $v = 1.67km/h$. That means the proposed differential scheme can work in some high mobility scenarios.

In Fig. 10, we consider a two-ray equal power delay profile with a delay of $\tau \mu s$ between the two rays to show the effects of diversity and channel permutation. Each OFDM modulator has $N_c = 128$ subcarriers with the total bandwidth of 1MHz. The corresponding OFDM block interval is $T = 128\mu s$ without the cyclic prefix. In this simulation, the fading channels are assumed to be constant within each OFDM block and changes independently from one OFDM block to another. $\tau = 1\mu s$ and $20\mu s$ are considered. Since the separation of $\tau = 1\mu s$ is very small compared with $T = 128\mu s$, the channel frequency responses change smoothly over different subcarriers, and the differential encoding is performed over adjacent subcarriers. We can see that the DSTFNC scheme performs successfully in this case. The effect of different Γ is investigated in

$$P(\mathbf{s}^k \rightarrow \mathbf{c}^k) \leq \prod_{n=1}^{N} \Big[\frac{4\varepsilon_n}{(1-\alpha)\sigma_n^2 |\mathbf{a}_n^{\mathrm{T}}\Delta\mathbf{s}|^2} \Big(\frac{P_t}{N_0} \Big)^{-1} - \sum_{m=1,m\neq n}^{N} \frac{C_M \xi_m}{\alpha \sigma_{mn}^2} \frac{4\varepsilon_n}{(1-\alpha)\sigma_n^2 |\mathbf{a}_n^{\mathrm{T}}\Delta\mathbf{s}|^2} \Big(\frac{P_t}{N_0} \Big)^{-2} + \sum_{l=1,l\neq n}^{N} \frac{C_M \xi_l}{\alpha \sigma_{ln}^2} \Big(\frac{P_t}{N_0} \Big)^{-1} + \text{H.O.T.} \Big]. \quad (43)$$

$$P(\mathbf{s}^k \rightarrow \mathbf{c}^k) \leq \prod_{n=1}^{N} \Big[\Big(\frac{P_t}{N_0} \Big)^{-1} \frac{1}{|\mathbf{a}_n^{\mathrm{T}}\Delta\mathbf{s}|^2} \Big(\frac{4\varepsilon_n}{(1-\alpha)\sigma_n^2} + \sum_{l=1,l\neq n}^{N} \frac{C_M \xi_l |\mathbf{a}_n^{\mathrm{T}}\Delta\mathbf{s}|^2}{\alpha \sigma_{ln}^2} \Big) \Big]. \quad (44)$$

Fig. 10. To compare with the same bit rate, QPSK is used for $\Gamma = 2$ and BPSK is used for $\Gamma = 1$. It is obvious that the BER performance with $\Gamma = 2$ is much better than that with $\Gamma = 1$ because higher diversity is achieved when $\Gamma = 2$, which exploits both spatial and frequency diversity. In case of $\tau = 20\mu s$, the channel frequency responses change severely. Therefore, as shown in Fig. 10, the DSTFNC scheme which differentially encoded over adjacent subcarriers fails to work. However, by utilizing the knowledge of statistical channel PDP, each user node can permutate the channel and obtain a smooth logical channel to guarantee the successful differential decoding. As shown by the curves with crosses and stars in Fig. 10, when $\Gamma = 1$, by channel permutation, the BER performance of $\tau = 20\mu s$ is almost the same as that of $\tau = 1\mu s$.

VI. CONCLUSION

In this paper, we consider the practical challenges in timing and frequency synchronization and channel estimation for multi-source cooperative communications and propose new cooperative differential transmission schemes for narrowband and broadband systems, called distributed DSTNC and DSTFNC, respectively, to overcome such issues. Compared with the traditional multi-source cooperative communication using TDMA, the proposed DSTNC can achieve full diversity with a significant reduction in transmission delay. The proposed schemes utilize linear network coding to combine the information and reduce the required time slot. The PEP performance of DSTNC is analyzed, and design criteria of the network coding vectors are derived. The performance with small channel coherence time is also studied to investigate the feasibility of DSTNC. The distributed DSTFNC is designed through mapping from DSTNC. The differential encoding is performed in frequency domain within each OFDM block. Despite the Doppler effects caused by mobility, the DSTFNC can still be decoded in high mobility scenarios. When the statistical channel PDP is known at the corresponding user node, the performance of the DSTFNC is improved by independent channel permutation at each user node. Simulation results are shown to validate our analysis.

APPENDIX

This appendix presents the proof of Theorem 1.

The SER for M-QAM modulation can be expressed as [35] $p_{mn} = F_2\Big(1 + \frac{b_q \gamma_{mn}}{\sin^2\theta}\Big)$, where $b_q = \frac{b_{QAM}}{2} = \frac{3}{2(M-1)}$ and γ_{mn} is the average received SNR at U_n for the symbols from U_m. γ_{mn} can be given as $\gamma_{mn} = \frac{\sigma_{mn}^2 P_I}{\xi_m N_0}$ where ξ_m has been

defined in Section II. B. The function $F_2(x(\theta))$ is given as [35]

$$F_2(x(\theta)) = \frac{4K}{\pi} \int_0^{\frac{\pi}{2}} \frac{1}{x(\theta)} d\theta - \frac{4K^2}{\pi} \int_0^{\frac{\pi}{4}} \frac{1}{x(\theta)} d\theta$$

with $K = 1 - \frac{1}{\sqrt{M}}$. Let C_M equal the following constant

$$C_M = \frac{4K}{\pi b_q} \int_0^{\frac{\pi}{2}} \sin^2\theta d\theta - \frac{4K^2}{\pi b_q} \int_0^{\frac{\pi}{4}} \sin^2\theta d\theta.$$

When SNR is high, $1 + \frac{b_q \gamma_{mn}}{\sin^2\theta} \approx \frac{b_q \gamma_{mn}}{\sin^2\theta}$ and p_{mn} can be approximated as

$$p_{mn} = C_M \gamma_{mn}^{-1}. \quad (42)$$

Let $\alpha = \frac{P_I}{P_t}$. Substituting (42) into (22) and ignoring the 1 in the denominator for high SNR, we can get (43) on the top of the this page. For high SNR, the term of $\Big(\frac{P_t}{N_0}\Big)^{-2}$ and H.O.T can be ignored. Then (43) becomes (44), which is shown on the top of the this page.

Because $\mathbf{a}_n^{\mathrm{T}}\mathbf{a}_n = 1$, the maximum value of $|\mathbf{a}_n^{\mathrm{T}}\Delta\mathbf{s}|$ is $\sqrt{N}d_{max}$, where d_{max} denotes the maximum Euclidean distance of $\mathcal{A}$. For example, if $\mathcal{A}$ is a 4-QAM constellation, the maximum can be achieved when $\Delta s_m = \sqrt{2}(1 + j)$, and $a_{mn} = \frac{1}{\sqrt{N}} e^{-j\frac{\pi}{4}}, m \in [1, N]$. Therefore, (44) can be upper bounded by

$$P(\mathbf{s}^k \rightarrow \mathbf{c}^k) < \prod_{n=1}^{N} \Big[\Big(\frac{P_t}{N_0} \Big)^{-1} \frac{1}{|\mathbf{a}_n^{\mathrm{T}}\Delta\mathbf{s}|^2} \Big(\frac{4\varepsilon_n}{\sigma_n^2} + \sum_{l=1,l\neq n}^{N} \frac{C_M \xi_l N d_{max}^2}{\sigma_{ln}^2} \Big) \Big]. \quad (45)$$

The upper bound in Theorem 1 is obtained.

REFERENCES

[1] J. N. Laneman, D. N. C. Tse, and G. W. Wornell, "Cooperative diversity in wireless networks: efficient protocols and outage behavior," *IEEE Trans. Inf. Theory*, vol. 50, no. 12, pp. 3062–3080, Dec. 2004.

[2] V. Tarokh, N. Seshadri, and A. R. Calderbank, "Space-time codes for high data rate wireless communication: performance criterion and code construction," *IEEE Trans. Inf. Theory*, vol. 44, no. 2, pp. 744–765, Mar. 1998.

[3] W. Su, X. G. Xia, and K. J. R. Liu, "A systematic design of high-rate complex orthogonal space-time block codes," *IEEE Commun. Lett.*, vol. 8, no. 6, pp. 380–382, 2004.

[4] J. N. Laneman and G. W. Wornell, "Distributed space-time-coded protocols for exploiting cooperative diversity in wireless network," *IEEE Trans. Inf. Theory*, vol. 49, no. 10, pp. 2415–2425, Oct. 2003.

[5] A. K. Sadek, W. Su, and K. J. R. Liu, "Multinode cooperative communications in wireless networks," *IEEE Trans. Signal Process.*, vol. 55, no. 1, pp. 341–355, Jan. 2007.

[6] Q. Zhao and H. Li, "Differential modulation for cooperative wireless systems," *IEEE Trans. Signal Process.*, vol. 55, no. 5, pp. 2273–2283, May 2007.

[7] Y. Shang and X. G. Xia, "Shift-full-rank matrices and applications in space-time trellis codes for relay networks with asynchronous cooperative diversity," *IEEE Trans. Inf. Theory*, vol. 52, no. 7, pp. 3153–3167, July 2006.

[8] M. O. Damen and A. R. Hammons, "Delay-tolerant distributed TAST codes for cooperative diversity," *IEEE Trans. Inf. Theory*, vol. 53, no. 10, pp. 3755–3773, Oct. 2007.

[9] S. Wei, D. Goeckel, and M. Valenti, "Asynchronous cooperative diversity," *IEEE Trans. Wireless Commun.*, vol. 5, no. 6, pp. 1547–1557, June 2006.

[10] M. Sharp, A. Scaglione, and B. Sirkeci-Mergen, "Randomized cooperation in asynchronous dispersive links," *IEEE Trans. Commun.*, vol. 57, no. 1, pp. 64–68, Jan. 2009.

[11] X. Li, "Space-time coded multi-transmission among distributed transmitters without perfect synchronization," *IEEE Signal Process. Lett.*, vol. 11, no. 12, pp. 948–951, Dec. 2004.

[12] A. Ribeiro, R. Wang, and G. B. Giannakis, "Multi-source cooperation with full-diverisy spectral-efficiency and controllable-complexity," *IEEE J. Sel. Areas Commun.*, vol. 25, no. 2, pp. 415–425, Feb. 2007.

[13] A. Cano, J. Gomez-Vilardebo, A. I. Perez-Neira, and G. B. Giannakis, "High-rate distributed multi-source cooperation using complex field coding," in *Proc. ICASSP*, Apr. 2009, pp. 2633–2636.

[14] H. Q. Lai, A. Ibrahim, and K. J. R. Liu, "Wireless network cocast: Location-aware cooperative communications with linear network coding," *IEEE Trans. Wireless Commun.*, vol. 8, no. 6, pp. 1–11, June 2009.

[15] H. Q. Lai and K. J. R. Liu, "Space-time network coding," *IEEE Trans. Signal Process.*, vol. 59, no. 4, pp. 1706–1718, Apr. 2011.

[16] Y. Jing and H. Jafarkhani, "Distributed differential space-time coding for wireless relay networks," *IEEE Trans. Commun.*, vol. 56, no. 7, pp. 1092–1100, July 2008.

[17] T. Himsoon, W. P. Siriwongpairat, W. Su, and K. J. R. Liu, "Differential modulation for multinode cooperative communications," *IEEE Trans. Signal Process.*, vol. 56, no. 7, pp. 2941–2956, July 2008.

[18] S. Y. R. Li, W. Yeung, and N. Cai, "Linear network coding," *IEEE Trans. Inf. Theory*, vol. 49, no. 2, pp. 371–381, Feb. 2003.

[19] E. Fasolo, F. Rossetto, and M. Zorzi, "Network coding meets MIMO," in *Proc. Workshop Network Coding, Theory, Appl.*, Jan. 2008, pp. 1–6.

[20] W. Su and K. J. R. Liu, "Differential space-frequency modulation via smooth logical channel for broadband wireless communications," *IEEE Trans. Commun.*, vol. 53, no. 12, pp. 2024–2028, Dec. 2005.

[21] M. Damen, A. Chkeif, and J. Belfiore, "Lattice code decoder for space-time codes," *IEEE Signal Process. Lett.*, vol. 4, no. 5, pp. 161–163, May 2000.

[22] Z. Safar, W. Su, and K. J. R. liu, "A fast sphere decoding framework for space-frequency block codes," in *Proc. ICC*, 2004, pp. 2591–2595.

[23] B. L. Hughes, "Differential space-time modulation," *IEEE Trans. Inf. Theory*, vol. 46, no. 7, pp. 2567–2578, Nov. 2000.

[24] B. M. Hochwald and T. L. Marzetta, "Unitary space-time modulation for multiple-antenna communications in Rayleigh flat fading," *IEEE Trans. Inf. Theory*, vol. 46, no. 2, pp. 543–564, Mar. 2000.

[25] V. Tarokh and H. Jafarkhani, "A differential detection scheme for transmit diversity," *IEEE J. Sel. Areas Commun.*, vol. 18, no. 7, pp. 1169–1174, July 2000.

[26] V. Tarokh, H. Jafarkhani, and A. R. Calderbank, "Spcae-time block codes from orthogonal design," *IEEE Trans. Inf. Theory*, vol. 45, no. 5, pp. 1456–1467, July 1999.

[27] X. Giraud, E. Boutillon, and J. C. Belfiore, "Algebraic tools to build modulation schemes for fading channels," *IEEE Trans. Inf. Theory*, vol. 43, no. 3, pp. 938–952, May 1997.

[28] J. Boutros and E. Viterbo, "Signal space diversity: a power and bandwith efficient diversity technique for the Rayleigh fading channel," *IEEE Trans. Inf. Theory*, vol. 44, no. 4, pp. 1453–1467, July 1998.

[29] W. Su, Z. Safar, and K. J. R. Liu, "Signal space diversity: a power and bandwith efficient diversity technique for the Rayleigh fading channel," *IEEE Trans. Wireless Commun.*, vol. 4, no. 4, pp. 1847–1857, July 2005.

[30] ——, "Full-rate full-diversity space-frequency codes with optimum coding advantage," *IEEE Trans. Inf. Theory*, vol. 51, no. 1, pp. 229–249, Jan. 2005.

[31] W. Su, Z. Safar, M. Olfat, and K. J. R. Liu, "Obtain full-diversity space-frequency codes from space-time codes via mapping," *IEEE Trans. Signal Process.*, vol. 51, no. 11, pp. 2905–2916, Nov. 2003.

[32] G. Gallo and S. Pallotino, "Shortest path methods: a unifying approach," *Math. Program. Study*, vol. 26, pp. 2905–2916, Nov. 1986.

[33] W. C. Jakes, *Microwave Mobile Communicationss*. Wiley-IEEE Press, 1994.

[34] Y. Chen, E. Aktas, and U. Tureli, "Optimal space-frequency group codes for MIMO-OFDM system," *IEEE Trans. Commun.*, vol. 54, no. 3, pp. 553–562, Mar. 2006.

[35] K. J. R. Liu, A. K. Sadek, W. Su, and A. Kwasinski, *Cooperative Communications and Networking*. Cambridge University Press, 2008.

Zhenzhen Gao (S'10) received the B.S. in communication engineering in 2005 from Lanzhou University, Lanzhou, China. She is now a Ph.D. student in the Department of Information and Communication Engineering, Xi'an Jiaotong University, Xi'an, China. She received a scholarship from the China Scholarship Council (CSC) in 2009. From September 2009 to August 2011, she was a visiting student in the Department of Electrical and Computer Engineering at the University of Maryland, College Park, MD, USA. Her current research interests are in the areas of wireless communications and networks, including cooperative communications, space-time coding, and network coding.

Hung-Quoc Lai (M'11) received the B.S. (cum laude) degree, the M.S. degree, and the Ph.D. degrees all in electrical engineering from the University of Maryland, College Park, Maryland in 2004, 2006, and 2011, respectively. Since 2006, he has been with the U.S. Army RDECOM CERDEC at Aberdeen Proving Ground, Maryland, where he currently is the Technical Lead in research areas of multiple-input multiple-output (MIMO) and cooperative communications. Dr. Lai is a Gates Millennium Scholar. He is the recipient of a university-level Distinguished Teaching Assistant Award from the University of Maryland and of the 2004-2005 George Corcoran Memorial Award, a lifetime award for his contributions to ECE education, the Department of Electrical and Computer Engineering, University of Maryland.

K. J. Ray Liu (F'03) became a Distinguished Scholar-Teacher of the University of Maryland, College Park, in 2007, where he is the Christine Kim Eminent Professor of Information Technology. He serves as Associate Chair of Graduate Studies and Research of the Electrical and Computer Engineering Department and leads the Maryland Signals and Information Group conducting research encompassing broad aspects of wireless communications and networking, information forensics and security, multimedia signal processing, and biomedical engineering.

Dr. Liu is the recipient of numerous honors and awards including the IEEE Signal Processing Society Technical Achievement Award and is a Distinguished Lecturer. He also received various teaching and research recognitions from the University of Maryland including the university-level Invention of the Year Award; and the Poole and Kent Senior Faculty Teaching Award and Outstanding Faculty Research Award, both from the A. James Clark School of Engineering. An ISI Highly Cited Author in Computer Science, Dr. Liu is a Fellow of IEEE and AAAS.

Dr. Liu is President-Elect and was Vice President - Publications of the IEEE Signal Processing Society. He was the Editor-in-Chief of *IEEE Signal Processing Magazine* and the the founding Editor-in-Chief of the *EURASIP Journal on Advances in Signal Processing*.